Open access • Journal Article • DOI:10.1109/TPEL.2010.2099133

Fault Ride-Through of a DFIG Wind Turbine Using a Dynamic Voltage Restorer During Symmetrical and Asymmetrical Grid Faults — Source link

C. Wessels, F. Gebhardt, Friedrich W. Fuchs

Institutions: University of Kiel

Published on: 01 Mar 2011 - IEEE Transactions on Power Electronics (IEEE)

Topics: Crowbar, Wind power, Turbine, Voltage regulator and Low voltage

Fault Ride Through of DFIG Wind Turbines during symmetrical voltage dip with Crowbar or Stator Current Feedback Solution

Christian Wessels, Student member, IEEE and Friedrich W. Fuchs, Senior member, IEEE
Institute of Power Electronics and Electrical Drives
Christian-Albrechts University of Kiel
Kaiserstrasse 2, 24143 Kiel, Germany
Email: chw@tf.uni-kiel.de, fwf@tf.uni-kiel.de

***Abstract*—Low Voltage Ride Through is an important feature for wind turbine systems to fulfill grid code requirements. In case of wind turbine technologies using doubly fed induction generators the reaction to grid voltage disturbances is sensitive. Hardware or software protection must be implemented to protect the converter from tripping during severe grid voltage faults. In this paper two methods for low voltage ride through of symmetrical grid voltage dips are investigated. As a basis, an analysis of the rotor voltages during grid fault is given. First, the conventional hardware method using a crowbar is introduced. Then the stator current reference feedback solution is presented. Both methods are investigated and compared by simulation results using 2 MW wind turbine system parameters. Measurement results on a 22 kW laboratory DFIG test bench show the effectiveness of the proposed control technique.**

I. Introduction

The increased amount of power from decentralised, renewable energy systems, as especially wind energy systems, requires strong grid code requirements to maintain a stable and safe operation of the energy network. The grid codes cover rules considering the fault ride through behaviour as well as the steady state active power and reactive power production. The actual grid codes stipulate that wind farms should contribute to power system control like frequency and voltage control to behave much as conventional power stations. A detailed review of grid code technical requirements regarding the connection of wind farms to the electrical power system is given in [1]. For operation during grid voltage faults it becomes clear that grid codes prescribe that wind turbines must stay connected to the grid and should support the grid by generating reactive power to support and restore quickly the grid voltage after the fault.

Among the wind turbine concepts turbines using the doubly fed induction generator (DFIG) as described in [2] and [3] and shown in Fig. 1 are dominant due to their variable speed operation, the separately controllable active and reactive power and their partially rated power converter. But, the reaction of DFIGs to grid voltage disturbances is sensitive, as described in [4] and [5] for symmetrical and unsymmetrical voltage dips, and requires additional protection for the rotor side power electronic converter.

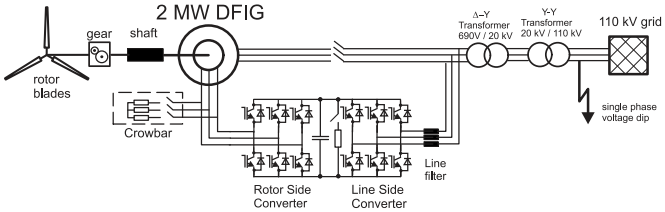

Fig. 1: Schematic diagram of DFIG wind turbine system

Conventionally a resistive network called crowbar is connected, in case of rotor overcurrents, to the rotor circuit and the rotor side converter is disabled as described in [6],[7],[8] and [9]. But the machine draws a high short circuit current when the crowbar is activated as described in [10] resulting in a large amount of reactive power drawn from the power network, which is not acceptable when considering grid code requirements. The lack of reactive power support capabilty when using crowbar circuits has led to a renewed interest for LVRT to ride through grid faults safely and fulfill the grid codes at the same time. There are several approaches limiting the rotor currents during transient grid voltage dip by changing the rotor side converters control without using external protection devices. The rotor side converter can be protected by feedforward of the faulty stator voltage [11], by considering the stator flux linkage [12] or other methods dealing with an improved control structure during unsymmetrical grid voltage conditions [13], [14] and [15]. In [16] a method, based on the conventional vector control, is proposed that aims to reduce the rotor currents by using the measured stator currents as reference for the current controllers. In this paper the stator current reference feedback solution [16] is investigated and compared to a conventional fault ride through of the DFIG using a crowbar cicuit. First results have been presented in [17] but detailed analysis is included here.

The paper is structured as follows. In section II the DFIG wind turbine concept is introduced. In chapter III an analysis of the rotorvoltage dynamics during nominal and during symmetrical grid volttage dip is given. Afterwards the rotor converter rating is taken into account. In chapter IV two solutions to protect

978-1-4244-5287-3/10/$26.00 ©2010 IEEE

the rotor converter are presented. First the hardware solution using a crowbar and then a software solution using the stator current feedback are presented. Simulation results for a 2 MW wind turbine in section V and measurement results on a 22 kW laboratory test bench in section VI show the effectiveness of the proposed technique in comparison to the LVRT of the DFIG using a crowbar. A conclusion closes the paper.

II. Doubly Fed Induction Generator

The investigated wind turbine system shown in Fig. 1 consists of the basic components like the turbine, a gearbox (in most systems), a DFIG generator and a back-to-back voltage source converter with a DC link. A DC chopper to limit the DC voltage across the DC capacitor and a crowbar are included. The back-to-back converter consists of a rotor side converter (RSC) and a line side converter (LSC) connected to the grid by a line filter to reduce the harmonics caused by the converter. The wind turbine system is connected to the high voltage grid by two transformers. Due to the short period of time of voltage disturbances the dynamics of the mechanical part of the turbine will be neglected and the mechanical torque brought in by the wind is assumed to be constant.

The RSC provides decoupled control of stator active and reactive power. A cascade vector control structure with inner current control loops is applied. The overall control structure is shown in Fig. 2.

III. DFIG Rotor Voltage Dynamics

A precise knowledge about amplitude and frequency of the rotor voltage is necessary to design and control the rotor side converter. Therefore equations for the rotor voltage in normal operation and under symmetrical stator voltage dip are derived in the following and in [5]. Afterwards the rotor converter rating is taken into account.

A. normal condition

From the per-phase equivalent circuit of the DFIG in a static stator oriented reference frame the following stator and rotor voltage and flux equations can be derived.

$$\vec{v}_s = R_s\vec{i}_s + \frac{d\vec{\psi}_s}{dt} \quad (1)$$

$$\vec{v}_r = R_r\vec{i}_r + \frac{d\vec{\psi}_r}{dt} - j\Omega\vec{\psi}_r \quad (2)$$

$$\vec{\psi}_s = L_s\vec{i}_s + L_h\vec{i}_r \quad (3)$$

$$\vec{\psi}_r = L_r\vec{i}_r + L_h\vec{i}_s \quad (4)$$

where $\vec{\psi}$, $\vec{v}$ and $\vec{i}$ represent the flux, voltage and current vectors respectively. Subscripts s and r denote the stator and rotor quantities respectively. $L_s = L_{s\sigma} + L_h$ and $L_r = L_{r\sigma} + L_h$ represent the stator and rotor inductance, L_h is the mutual inductance, R_s and R_r are the stator and rotor resistances and Ω is the rotor electrical speed (number of pole pairs multiplied by ω_{mech}).

By introducing the leakage factor $\sigma = 1 - \frac{L_h^2}{L_s L_r}$ the rotor flux can be described in dependence of the rotor current and the stator flux

$$\vec{\psi}_r = \frac{L_h}{L_s}\vec{\psi}_s + \sigma L_r\vec{i}_r \quad (5)$$

By substituting (5) in (2) an equation for the rotor voltage can be obtained,

$$\vec{v}_r = \frac{L_h}{L_s}\left(\frac{d}{dt} - j\Omega\right)\vec{\psi}_s + \left(R_r + \sigma L_r\left(\frac{d}{dt} - j\Omega\right)\right)\vec{i}_r \quad (6)$$

that consists of two parts. The first part is caused by the stator flux $\vec{\psi}_s$ that is given in normal operation by the constantly rotating vector:

$$\vec{\psi}_s = \frac{V_s}{j\omega_s}e^{j\omega_s t} \quad (7)$$

The second part of (6) is caused by the rotor current $\vec{i}_r$. The rotor resistance R_r and the leakage factor σ are often small, so the rotor voltage does not differ considerably from the part caused by the stator flux. Thus, the amplitude of the rotor voltage in normal condition V_{r0} can be calculated as

$$V_{r0} \approx V_s\frac{L_h}{L_s}\frac{\omega_r}{\omega_s} = V_s\frac{L_h}{L_s}s \quad (8)$$

where $s = 1 - (\Omega/\omega_s) = \omega_r/\omega_s$ describes the slip and ω_r the rotor frequency.

B. Symmetrical Voltage Dip, Constant Phase Angle

Under a symmetrical voltage dip the stator voltage is reduced from normal amplitude V_1 to the faulty amplitude V_2 as described in (9).

$$\vec{v}_s = \begin{cases} V_1 e^{j\omega_s t} & \text{for } t < t_0 \\ V_2 e^{j\omega_s t} & \text{for } t \geq t_0 \end{cases} \quad (9)$$

$$\vec{\psi}_s = \begin{cases} \vec{\psi}_{s1} = \frac{V_1}{j\omega_s}e^{j\omega_s t} & \text{for } t < t_0 \\ \vec{\psi}_{s2} = \frac{V_2}{j\omega_s}e^{j\omega_s t} & \text{for } t \geq t_0 \end{cases} \quad (10)$$

Since the stator flux is a continuous value it cannot follow the step function of the voltage. The evolution of the stator flux can be derived by solving the differential equation (11)

$$\frac{d\vec{\psi}_s}{dt} = \vec{v}_s - \frac{R_s}{L_s}\vec{\psi}_s \quad (11)$$

that can be derived from (1) and (3). Due to the low influence of the rotor current on the rotor voltage the open rotor condition is assumed ($\vec{i}_r = 0$). The solution consists of two parts. The first part is the steady state stator flux after the voltage dip, which is described by $\vec{\psi}_{s2}$ and the second part is the transition of the flux from $\vec{\psi}_{s1}$ to $\vec{\psi}_{s2}$ that is described by (12)

$$\vec{\psi}_s = \vec{\psi}_{s,diff}e^{-tR_s/L_s} = \vec{\psi}_{s,diff}e^{-t/\tau_s} \quad (12)$$

where $\vec{\psi}_{s,diff}$ is the difference of the stator flux before and after the voltage dip, described by $(V_1 - V_2)/j\omega_s$. Summarizing, the stator flux is given by the sum of the two parts:

$$\vec{\psi}_s(t) = \frac{V_2}{j\omega_s}e^{j\omega_s t} + \frac{V_1 - V_2}{j\omega_s}e^{-t/\tau_s} \quad (13)$$

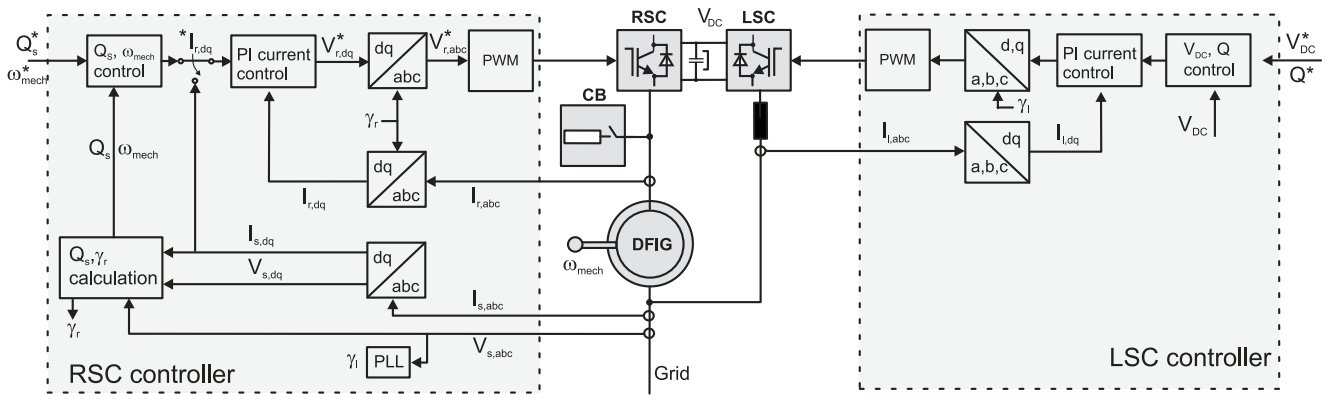

Fig. 2: Schematic diagram of DFIG wind turbine control structure

When the dynamic stator flux from (13) is considered in the rotor voltage equation of (6) (neglecting $\vec{i}_r$ and $1/\tau_s$) the dynamic behavior of the rotor voltage under symmetrical voltage dip is described by (15)

$$\vec{v}_r = \frac{L_h}{L_s}\left(\frac{d}{dt} - j\Omega\right)\left(\frac{V_2}{j\omega_s}e^{j\omega_s t} + \frac{V_1 - V_2}{j\omega_s}e^{-t/\tau_s}\right) \quad (14)$$

$$= \frac{L_h}{L_s}\left(sV_2 e^{j\omega_s t} - (1-s)(V_1 - V_2)e^{-t/\tau_s}\right) \quad (15)$$

In a reference frame rotating at rotor frequency the following rotor voltage is obtained:

$$\vec{v}_r = \frac{L_h}{L_s}\left(sV_2 e^{j\omega_r t} - (1-s)(V_1 - V_2)e^{-j\Omega t}e^{-t/\tau_s}\right) \quad (16)$$

The results of this analysis show that the rotor voltage during symmetrical voltage dip consists of two components. The first part is proportional to the slip and the remaining stator voltage, thus for a deep voltage dip and a slip usually at -0.2 it is small. The frequency of the first part is the slip frequency (at a slip of -0.2 ω_r = 10 Hz). The second part of (16) has a high amplitude at t=0 proportional to (1-s) and rotates at the mechanical frequency Ω (at a slip of -0.2: Ω = 60 Hz). The term is decaying exponentially with the stator time constant of τ_s. The maximum rotor voltage during symmetrical voltage dip will occur at the beginning of the fault (t=0) and for a full dip (V_2 = 0)

$$V_{rmax} = \frac{L_h}{L_s}(1-s)V_1 \quad (17)$$

C. Rotor Side Converter Rating

The nominal power of the rotor side converter of a DFIG is rated for a part of the stator power because the rotor power is approximately proportional to the slip

$$P_{r,n} \approx sP_{s,n} \quad (18)$$

that is chosen usually for wind turbine systems to $s = \pm 0.3$. The required amplitude of the rotor voltage is probably determined (with $L_h/L_s \approx 1$ in (8)) by

$$V_r = sV_s/N_{sr} \quad (19)$$

where N_{sr} is the stator to rotor turns ratio. The turns ratio is usually set at 1/2 or 1/3 in practical wind turbine driven DFIGs to make full use of the DC link voltage and reduce the converters current rating. The required DC link voltage can be determined by

$$V_{conv} = m\frac{V_{DC}}{2} = V_r \quad (20)$$

where m is the modulation index of the pulse width modulation (PWM) technique. The maximum value of the modulation index is 1.0 for the carrier based sinusoidal PWM and 1.15 for the space vector modulation, both without overmodulation techniques [18].

The findings of the section enhance the understanding of rotor overcurrents during symmetrical grid voltage dip. Only if the rotor side converter can provide a sufficient voltage level controllability of rotor currents can be obtained. If the rotor voltage exceeds the converter voltage high currents will flow through the diodes into the dc link capacitor, damaging the IGBT or the DC capacitor.

IV. DFIG Protection

A. Crowbar

To protect the rotor side converter from tripping due to overcurrents in the rotor circuit or overvoltage in the DC link during grid voltage dips a crowbar is installed in conventional DFIG wind turbines, which is a resistive network that is connected to the rotor windings of the DFIG. The crowbar limits the voltages and provides a safe route for the currents by bypassing the rotor by a set of resistors. When the crowbar is activated the rotor side converters pulses are disabled and the machine behaves like a squirrel cage induction machine directly coupled to the grid. The magnetization of the machine that was provided by the RSC in nominal condition is lost and the machine absorbs a large amount of reactive power from the stator and thus from the network [10], which can further reduce the voltage level and is not allowed in actual grid codes. Triggering of the crowbar circuit also means high stress to the mechanical components of the system as the shaft and the gear. Detailed analyses on the DFIG behavior during voltage

dip and crowbar protection can be found in [6] and [10]. Thus, from network and from machine mechanical point of view a crowbar triggering should be avoided.
Anyway, to compare the presented technique here with a conventional DFIG wind turbine system protected by a crowbar circuit, simulation results including crowbar protection are examined. Therefore the crowbar resistance is designed here. Crowbar resistances are also designed in [9] and [10], but here the resistance design is based on the analytical findings on the rotor voltage from the previous section.
There are two constraints that give an upper and a lower limit to the crowbar resistance. As a first constraint the crowbar resistance should be high enough to limit the short circuit rotor current $I_{r,max}$. If the crowbar is activated, the crowbar resistance R_{cb} is added to the rotor circuit, resulting in the maximum rotor current of (if R_r is neglected)

$$I_{r,max} = \frac{V_{rmax}}{\sqrt{X_{\sigma r}^2 + R_{cb}^2}} \tag{21}$$

If the maximum rotor voltage during grid voltage dip from (17) is considered the minimum crowbar resistance can be derived as:

$$R_{cb,min} = \sqrt{\left(\frac{L_h}{L_s}\frac{(1-s)V_1}{I_{r,max}}\right)^2 - {X_{\sigma r}}^2} \tag{22}$$

As the second constraint, the crowbar resistance should be low enough to avoid too high voltage in the rotor circuit. If the voltage across the crowbar terminals rises above the maximum converter voltage high currents will flow through the antiparallel diodes of the converter. A crowbar resistance of $R_{crow} = 150R_r$ is used in the simulations. Simulation results for different crowbar resistances during a 10% voltage dip is shown in Fig. 3. There are approaches limiting the operation

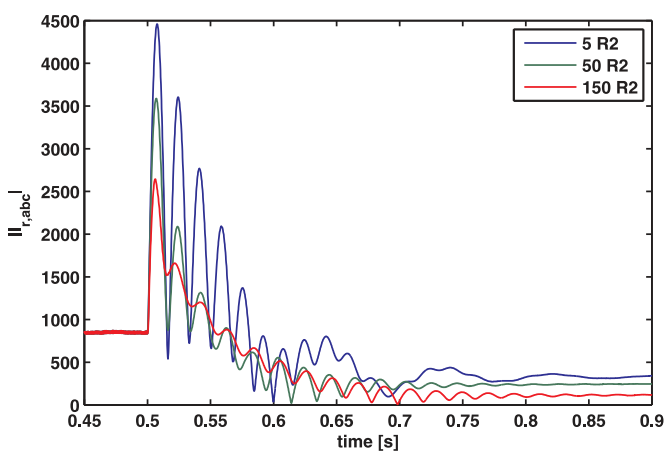

Fig. 3: Simulated rotor current during 10% voltage dip with crowbar activated at t=0.5 s

time of the crowbar to return to normal DFIG operation with active and reactive power control as soon as possible. A hysteresis control triggered by the rotor current is presented in [8] and also applied in the simulations here. A reset of the integral values of the RSCs current and power control before restart is necessary to avoid overcurrents.
In the laboratory setup a passive crowbar circuit is used that is triggered by a rotor overcurrent. The crowbar can be disabled manually by the user when safe circumstances are reestablished.

B. Stator Current Feedback Solution

The proposed technique aims to reduce the rotor currents by changing the RSC control instead of installing additional hardware protection like a crowbar in the wind turbine system. The solution has been presented in [16]. When a fault affects the generator the measured and transformed stator currents are fed back as reference for the rotor current controller (stator currents in stator flux orientation). The objective is to reduce stator current oscillations and thus reduce the rotor currents as well.
If the DFIG system equations (1)-(4) are combined, a Lapace transformation is performed and some simplifications are assumed, the following equation for the stator currents can be obtained:

$$i_{sd} = \frac{1}{L_s}\frac{\omega_s}{s^2 + 2(R_s/L_s)s + \omega_s^2}v_{sq} - \frac{L_h}{L_s}i_{rd} \tag{23}$$

$$i_{sq} = \frac{1}{L_s}\frac{s + R_s/L_s}{s^2 + 2(R_s/L_s)s + \omega_s^2}v_{sq} - \frac{L_h}{L_s}i_{rq} \tag{24}$$

If the stator currents are fed back as rotor current reference values, i.e. $i_{rd}^* = i_{sd}$ and $i_{rq}^* = i_{sq}$ the following equation for the stator currents can be obtained and the stator currents are reduced.

$$i_{sd} = \frac{1}{L_s + L_h}\frac{\omega_s}{s^2 + 2(R_s/L_s)s + \omega_s^2}v_{sq} \tag{25}$$

$$i_{sq} = \frac{1}{L_s + L_h}\frac{s + R_s/L_s}{s^2 + 2(R_s/L_s)s + \omega_s^2}v_{sq} \tag{26}$$

The most important limitation lies in the fact that the rotor converter voltage (20) must at least be as high as the maximum rotor voltage during voltage dip (17) to contain current controllability. If current controllability is assured, the stator current feedback solution can reduce stator currents thus rotor currents effectively. Otherwise, if the rotor voltages exceed the converter voltages, in case of deep voltage dips, hardware protection solutions as the crowbar must be applied.

V. Simulation Results

To show the effectiveness of the proposed technique simulations have been performed using MATLAB/Simulink and PLECS for a 2 MW DFIG wind turbine system as shown in Fig. 1. The simulation parameter are given in table I. The control structure as shown in Fig. 2 is implemented. The system performance of the DFIG is shown in Fig. 4 protected by the conventional crowbar and in Fig. 5 protected by the stator current feedback solution during a three phase 50 % voltage dip of 100 ms duration at the medium voltage level (20 kV) (see Fig. 4,5 a)).
The DFIG reacts to the three phase voltage dip with high stator currents I_s and thus high rotor currents are induced in the rotor

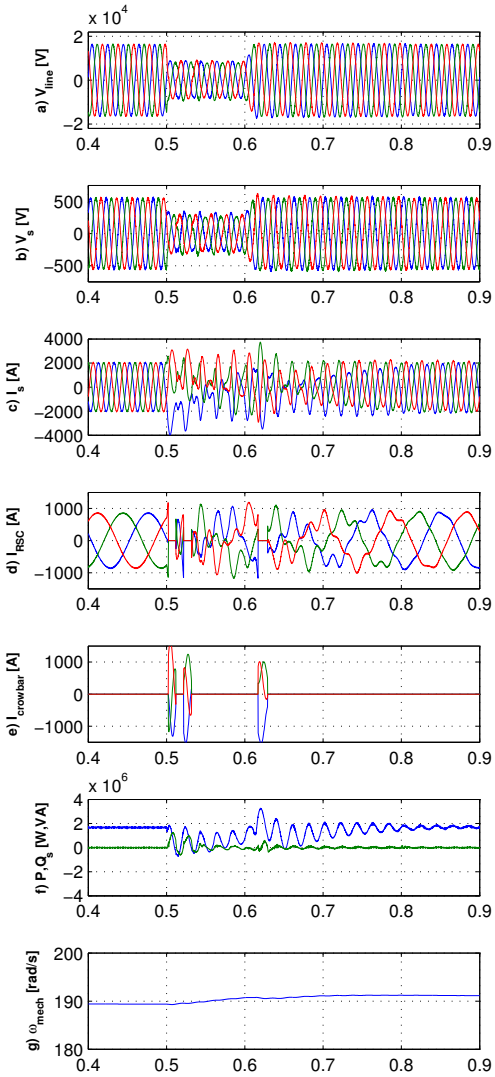

Fig. 4: DFIG performance with Crowbar protection during 50 % three phase voltage dip
a) Line voltage b) Stator voltage c) Stator current
d) Rotor side converter current e) Crowbar current
f) Active and reactive stator power g) mechanical speed

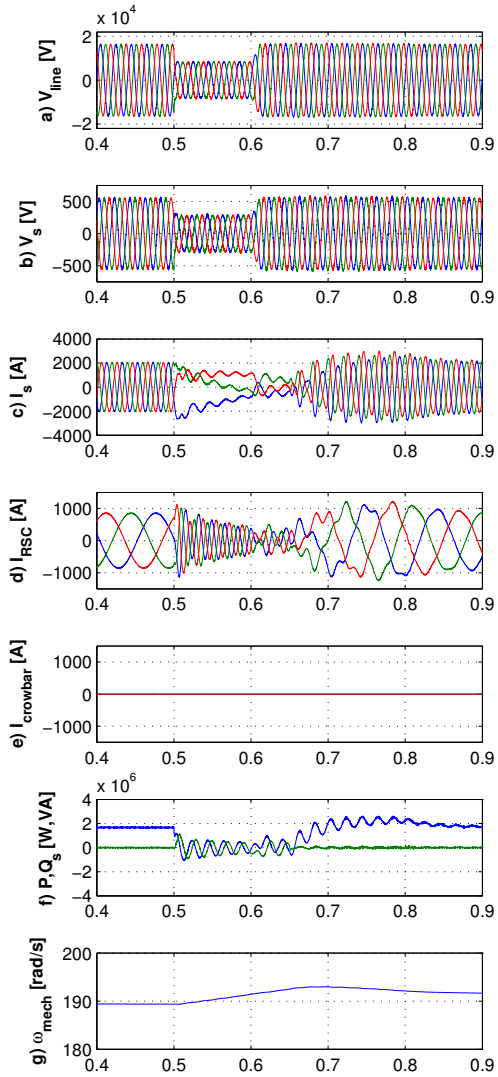

Fig. 5: DFIG performance with stator current reference protection during 50 % three phase voltage dip
a) Line voltage b) Stator voltage c) Stator current
d) Rotor side converter current e) Crowbar current
f) Active and reactive stator power g) mechanical speed

circuit. When the rotor currents exceed the maximum level of the hysteresis crowbar ($I_{r,max} = 1400A$) control the crowbar is triggered to protect the RSC from overcurrents I_{RSC} (Fig. 4 d),e)). The crowbar has to be triggered several times during the voltage dip. When the RSC is in operation the machine magnetization is provided by the rotor but every time the crowbar is triggered the RSC is disabled and the machine is excited by the stator. Thus, continuous reactive power control cannot be provided during the voltage dip (see Fig. 4 f)) which is not acceptable when considering the grid codes. The active power is oscillating as well so that a constant speed can not be ensured.

In Fig. 5 the wind turbine system is protected by the proposed stator current feedback solution. The rotor currents are reduced

during grid voltage dip and thus no crowbar triggering is necessary any more. The stator currents decay slowly having a DC component. The RSC can stay in operation. When the stator current feedback is activated the outer power control loops are disabled and thus active and reactive power control are not achieved. The power control can be implemented to fulfil grid code requirements when the transients have decayed. After fault clearance the wind turbine system can continue with nominal operation.

VI. Measurement Results

Measurement results are taken at a 22 kW DFIG wind turbine test bench similar to the one shown in Fig. 1 but the transformers are not included. Experimental setup parameters are given in table I. Both the RSC and the LSC are 2-level PWM converters consisting of IGBT modules connected to a DC capacitor. The DFIG is driven by an industrial 18,5 kW induction machine drive to emulate the wind. For all experimental tests the DFIG is operated supersynchronous with a slip of s=-0,2 (mechanical speed of 1800 r/min). The three phase grid voltage dips are generated by a transformer based voltage sag generator as described in [19].
Overvoltages are induced in the rotor circuit during a 12,5 % symmetrical stator voltage dip of 400 ms duration as shown in Fig. 6 where the rotor voltages in open rotor experiment (i.e. the RSC is not in operation) are shown. The induced voltages decay with a time constant of $\tau_s = L_s/R_s$ and have a frequency of ω_{mech}=40 Hz (here 20% slip) superimposed to the slip frequency of ω_{slip} = 10 Hz which is described in detail in [4]. These overvoltages cause overcurrents in the rotor circuit, if the RSC is in operation.

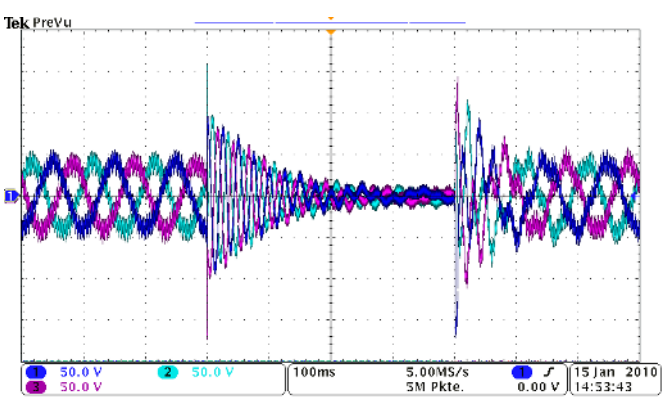

Fig. 6: Open rotor experiment: Rotor voltages during symmetrical 12,5 % voltage dip of 400 ms duration

The DFIG reaction to a symmetrical voltage dip when the RSC is in operation is shown in the following figures. Before the voltage dip the DFIG is feeding an active stator power of P_s=10 kW to the grid. Rotor overcurrents cause a triggering of the crowbar circuit at t=-160 ms shown in figure 7. In the laboratory experiment a passive crowbar is implemented (crowbar is not deactivated during voltage dip). Rotor currents are flowing in the crowbar and are reduced, but high stator currents are produced. These experimental results do not match the simulation results very well because in the simulations an active crowbar is implemented.

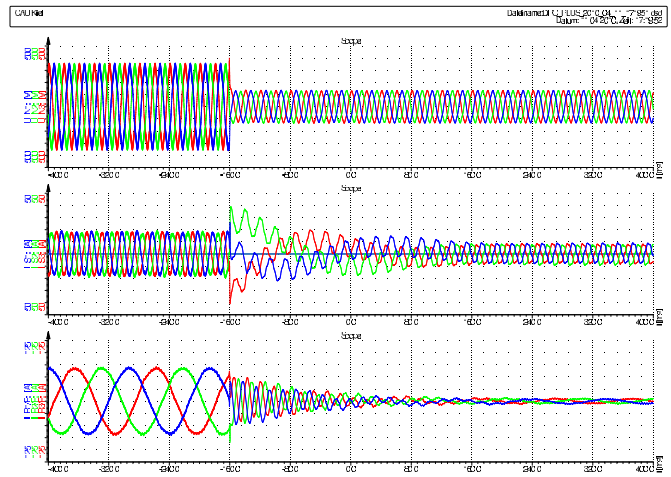

Fig. 7: Measurement results of DFIG LVRT with passive Crowbar during symmetrical 37 % voltage dip; upper:stator voltages, middle: stator currents lower: rotor currents

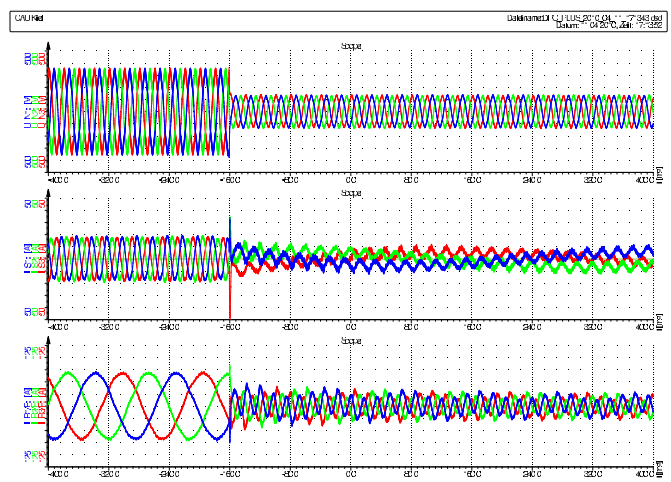

Fig. 8: Measurement results of DFIG LVRT with stator current feedback solution during symmetrical 37 % voltage dip; upper:stator voltages, middle: stator currents lower: rotor currents

When the DFIG is protected by the stator current feedback solution (Fig. 8) rotor and stator currents can be reduced during grid voltage dip with the RSC in operation. No overcurrents in stator or rotor are produced. Similar behaviour as in the simulations can be found. The stator currents contain DC components, but no overcurrents can be found.
Note, that the stator to rotor transmission ratio of the laboratory machine is 1/0.66 which helps to further reduce the induced rotor voltages by the stator voltage dip. The rotor side converter operates with a maximum converter voltage above the maximum rotor voltages during dip so that current

controllability is always contained in the laboratory setup. In a wind turbine system stator to rotor transmission ratios of 1/2 or 1/3 are usually chosen, making rotor voltages even higher which makes it challenging to obtain the current controllability.

In future investigations the implementation of grid services as reactive power production during voltage dip can be implemented.

VII. Conclusion

Low Voltage Ride Through is an important feature for wind turbine systems to fulfill grid code requirements. In case of wind turbine technologies using doubly fed induction generators the reaction to grid voltage disturbances is sensitive. Hardware or software protection must be implemented to protect the converter from tripping during severe grid voltage faults. In this paper two methods for LVRT are investigated. The first solution is the conventionally used crowbar circuit which is a resistive network connected to the rotor circuit. To avoid the disadvantages of crowbar operation such as reactive power consumption the stator current reference feedback solution is investigated. Limitations of the method are derived by an analysis of the DFIG rotor voltage and converter capabilities. The most important limitation lies in the fact that the rotor converter voltage must at least be as high as the maximum converter voltage during voltage dip to contain current controllability. Simulations of a 2 MW wind turbine system and measurement results of a 22 kW laboratoty DFIG test bench are presented to show the effectiveness of the proposed method. When the transients have decayed special grid services such as reactive power production during grid voltage fault can be implemented.

TABLE I: Simulation and experimental parameter

Simulation Parameters		
Symbol	Quantity	Value
U_{line}	low voltage level	690 V
U_{line}	medium voltage level	20 kV
ω	Line angular frequency	2 π 50 Hz
P_{DFIG}	Wind turbine rated power	2 MW
N_{sr}	stator to rotor transmission ratio	1/2.5
n	Rated speed	1800 r/min
Experimental Parameters		
Symbol	Quantity	Value
U_{line}	grid voltage (phase-to-phase, rms)	400 V
ω_s	Line angular frequency	2 π 50 Hz
P_{DFIG}	DFIG rated power	22 kW
P_{test}	DFIG experimental test power	10 kW
n_{mech}	Operation speed	1800 r/min
N_{sr}	stator to rotor transmission ratio	1/0.66
L_h	mutual inductance	37,13 mH
$L_{s\sigma}$	stator stray inductance	1,295 mH
$L'_{r\sigma}$	rotor stray inductance	0,431 mH
$R_{crowbar}$	crowbar resistance	2,7 Ω
V_{DC}	back-to-back converters DC voltage	320 V
C_{DC}	DC link capacitance	8 mF
f_s	switching frequency LSC and RSC	5 kHz

References

[1] M. Tsili and S. Papathanassiou, "A review of grid code technical requirements for wind farms," *Renewable Power Generation, IET*, vol. 3, no. 3, pp. 308–332, Sept. 2009.

[2] R. Pena, J. Clare, and G. Asher, "Doubly fed induction generator using back-to-back pwm converters and its application to variable-speed wind-energy generation," *Electric Power Applications, IEE Proceedings -*, vol. 143, no. 3, pp. 231–241, May 1996.

[3] S. Muller, M. Deicke, and R. De Doncker, "Doubly fed induction generator systems for wind turbines," *Industry Applications Magazine, IEEE*, vol. 8, no. 3, pp. 26–33, May/Jun 2002.

[4] J. Lopez, P. Sanchis, X. Roboam, and L. Marroyo, "Dynamic behavior of the doubly fed induction generator during three-phase voltage dips," *Energy Conversion, IEEE Transactions on*, vol. 22, no. 3, pp. 709–717, Sept. 2007.

[5] J. Lopez, E. Gubia, P. Sanchis, X. Roboam, and L. Marroyo, "Wind turbines based on doubly fed induction generator under asymmetrical voltage dips," *Energy Conversion, IEEE Transactions on*, vol. 23, no. 1, pp. 321–330, March 2008.

[6] S. Seman, J. Niiranen, and A. Arkkio, "Ride-through analysis of doubly fed induction wind-power generator under unsymmetrical network disturbance," *Power Systems, IEEE Transactions on*, vol. 21, no. 4, pp. 1782–1789, Nov. 2006.

[7] S. Foster, L. Xu, and B. Fox, "Behaviour and protection of doubly-fed induction generators during network faults," in *Power & Energy Society General Meeting, 2009. PES '09. IEEE*, July 2009, pp. 1–8.

[8] L. Peng, B. Francois, and Y. Li, "Improved crowbar control strategy of dfig based wind turbines for grid fault ride-through," *Applied Power Electronics Conference and Exposition, 2009. APEC 2009. Twenty-Fourth Annual IEEE*, pp. 1932–1938, Feb. 2009.

[9] W. Zhang, P. Zhou, and Y. He, "Analysis of the by-pass resistance of an active crowbar for doubly-fed induction generator based wind turbines under grid faults," *Electrical Machines and Systems, 2008. ICEMS 2008. International Conference on*, pp. 2316–2321, Oct. 2008.

[10] J. Morren and S. de Haan, "Short-circuit current of wind turbines with doubly fed induction generator," *Energy Conversion, IEEE Transactions on*, vol. 22, no. 1, pp. 174–180, March 2007.

[11] J. Liang, W. Qiao, and R. Harley, "Direct transient control of wind turbine driven dfig for low voltage ride-through," in *Power Electronics and Machines in Wind Applications, 2009. PEMWA 2009. IEEE*, June 2009, pp. 1–7.

[12] D. Xiang, L. Ran, P. Tavner, and S. Yang, "Control of a doubly fed induction generator in a wind turbine during grid fault ride-through," *Energy Conversion, IEEE Transactions on*, vol. 21, no. 3, pp. 652–662, Sept. 2006.

[13] O. Gomis-Bellmunt, A. Junyent-Ferre, A. Sumper, and J. Bergas-Jan, "Ride-through control of a doubly fed induction generator under unbalanced voltage sags," *Energy conversion, IEEE Transactions on*, vol. 23, no. 4, pp. 1036–1045, Dec. 2008.

[14] L. Xu, "Coordinated control of dfig's rotor and grid side converters during network unbalance," *Power Electronics, IEEE Transactions on*, vol. 23, no. 3, pp. 1041–1049, May 2008.

[15] J. Hu, Y. He, L. Xu, and B. Williams, "Improved control of dfig systems during network unbalance using pir current regulators," *Industrial Electronics, IEEE Transactions on*, vol. 56, no. 2, pp. 439–451, Feb. 2009.

[16] K. Lima, A. Luna, P. Rodriguez, E. Watanabe, R. Teodorescu, and F. Blaabjerg, "Doubly-fed induction generator control under voltage sags," *Energy 2030 Conference, 2008. ENERGY 2008. IEEE*, pp. 1–6, Nov. 2008.

[17] C. Wessels and F. W. Fuchs, "Lvrt of dfigwind turbines - crowbar vs. stator current feedback solution -," in *EPE Wind Energy Chapter 2010, Symposium on*, April 2010.

[18] M. P. Kazmierkowski, R. Krishnan, F. Blaabjerg, and D. Irwin, *"Control in power electronics: selected problems"*, ser. "Academic Press series in engineering". "New York, NY": "Academic Press", "2002".

[19] C. Wessels, T. Wehrend, and F. W. Fuchs, "Transformer based voltage sag generator to test renewable energy systems during grid faults in the laboratory," in *EPE Wind Energy Chapter Symposium 2010*, April 2010.